

*ExB Workshop
November 1, 2018
Princeton, NJ*



MORE ON 1D AZIMUTHAL AND 2D R-THETA SIMULATIONS

Ken Hara¹, Ian DesJardin², Rob Martin³

¹ Texas A&M University;

² University at Buffalo (NSF-REU summer student at TAMU);

³ Air Force Research Laboratory, Edwards AFB

PIC simulation of electron cyclotron drift Instability (ECDI)

- Kinetic simulations, e.g., particle-in-cell (PIC) simulations, are useful in understanding the electron transport due to electron cyclotron drift instability (ECDI).
 - Collisionless scattering of electrons from azimuthal plasma waves
 - Good numerical test cases to *benchmark* codes (LANDMARK)
 - Such kinetic simulations can serve as a *validation* tool with advanced experimental measurements (e.g., laser diagnostics)
- We are interested in the *numerical effects* of the simulations proposed by others (Lafleur, Janhunen, Boeuf, etc.)

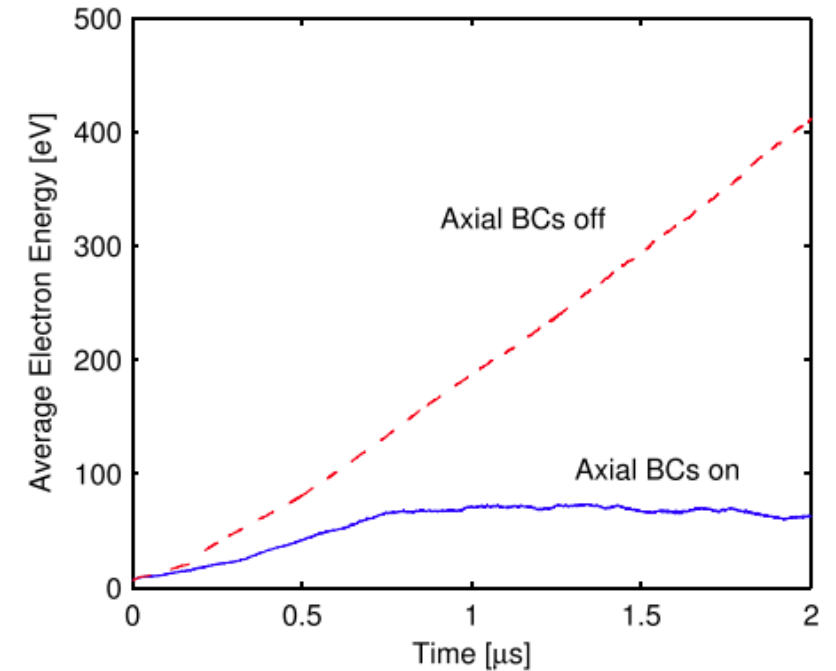
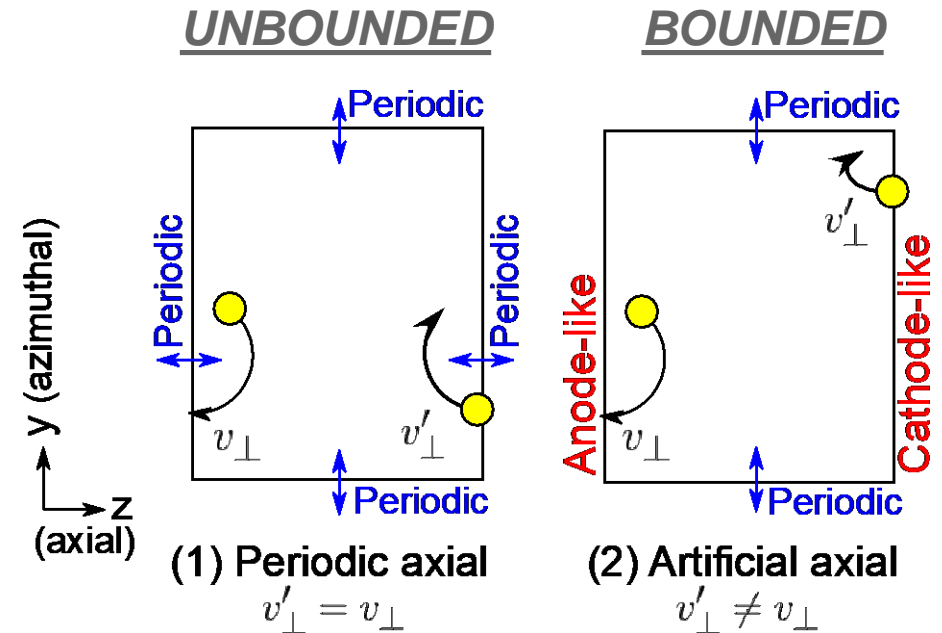


FIG. 8. Average electron energy as a function of time for a simulation with (a) “axial” boundary conditions imposed and (b) “axial” boundary conditions removed. The plasma density is $n_0 = 1 \times 10^{17} \text{ m}^{-3}$ and the neutral xenon pressure is zero.

Lafleur, T., et al. “Theory for the Anomalous Electron Transport in Hall Effect Thrusters. I. Insights from Particle-in-Cell Simulations.” *Physics of Plasmas*, vol. 23, no. 5, 2016, p. 053502., doi:10.1063/1.4948495.

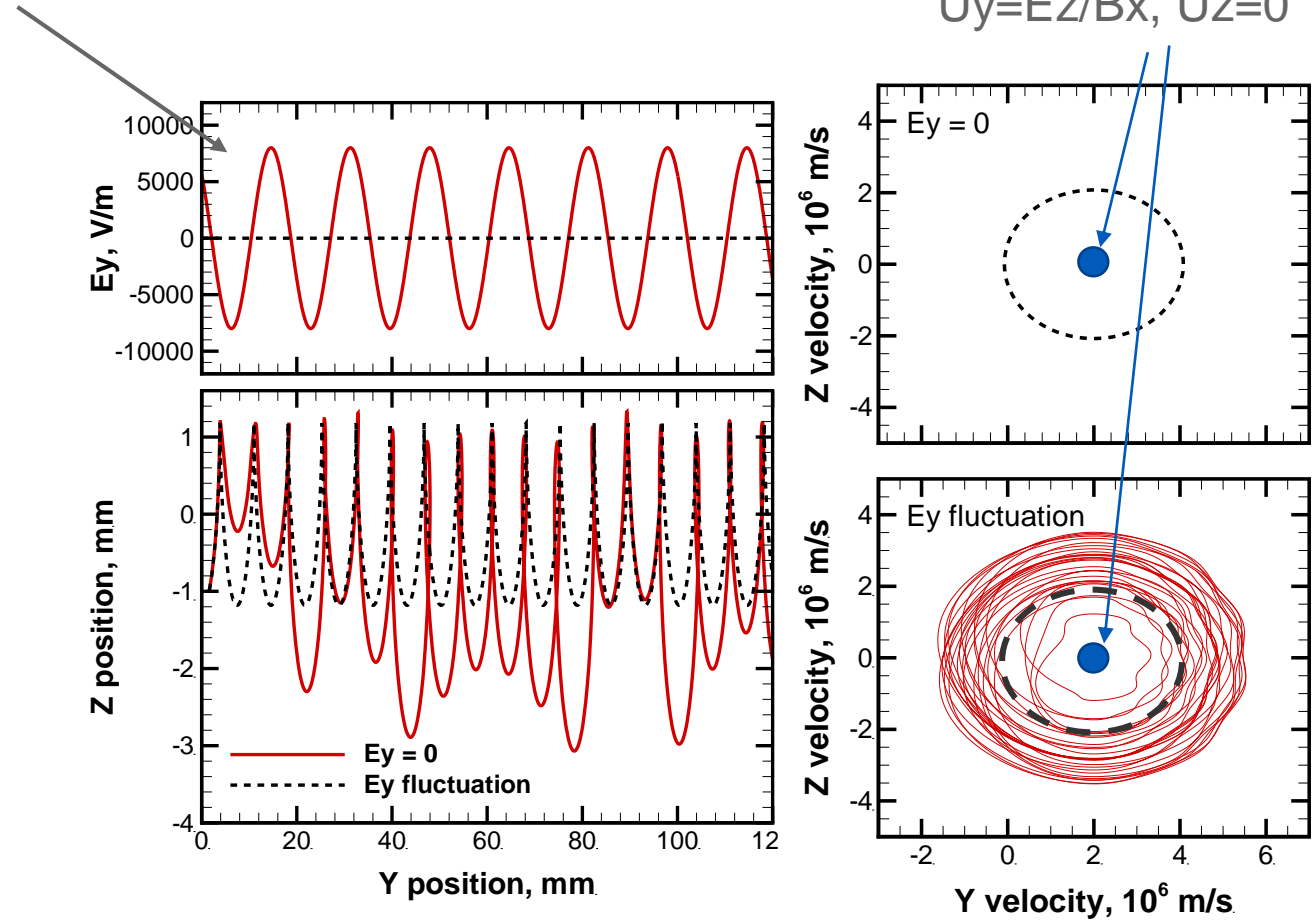
Numerical setup of the azimuthal PIC simulations

- A few numerical setups have been suggested.
 - Periodic axial (**unbounded**) case [Janhunen et al. PoP 2018]
 - Artificial axial (**bounded**) case: particles are *randomized* (effectively adding collisionality) in position & velocity [Lafleur et al. PoP 2016]
 - Realistic 2D (z-theta) case
 - 2D (r-theta) case
 - 3D (r-z-theta) case
- Two mechanisms need to be investigated.
 1. The source of azimuthal plasma wave (ECDI): **Studied.**
 2. The effect of azimuthal plasma wave to the cross-field electron transport: ***a bit more to do?***



The effect of azimuthal plasma wave to the cross-field electron transport

- Single particle theory in the presence of E_y fluctuation: $E_y = E_0 \cos(ky) + \text{constant } E_z$ and B_x
- Equations of motion
 - $\frac{dz}{dt} = v_z$; $\frac{dv_z}{dt} = \frac{q}{m} (E_z - v_y B_x)$
 - $\frac{dy}{dt} = v_y$; $\frac{dv_y}{dt} = \frac{q}{m} [E_y(y) + v_z B_x]$
- Observations
 - Chaotic trajectory in phase space \rightarrow electron heating
 - Guiding center motion (constant drift)? Shift in guiding center because of heating?



$$U_y = E_z / B_x, \quad U_z = 0$$

$E_y = 0$

E_y fluctuation

Benchmark against long-domain modulational instability due to ECDI [Janhunen et. al PoP 2018]

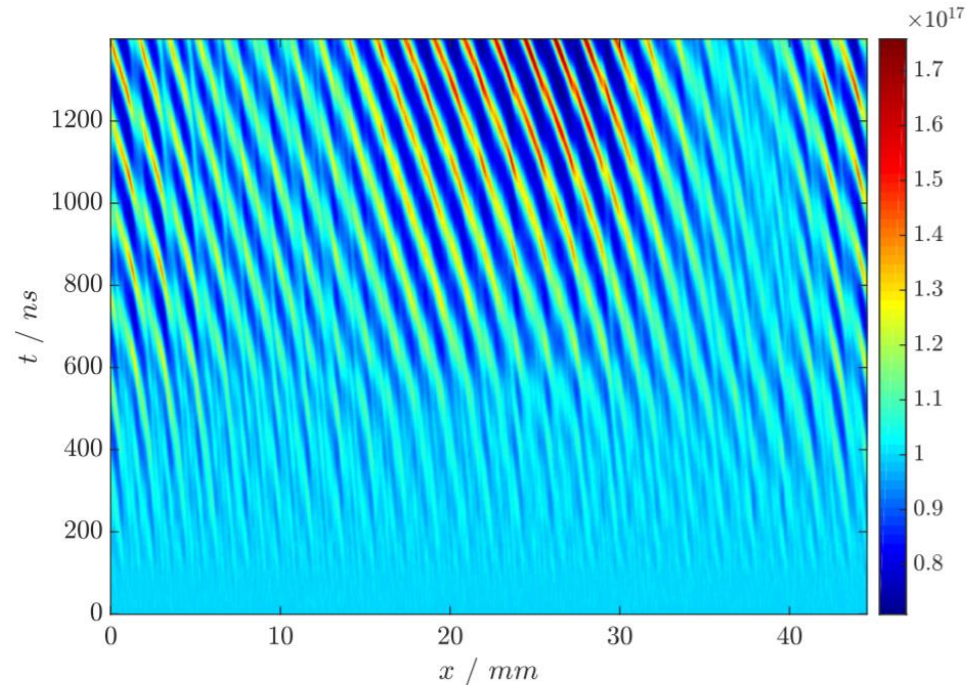
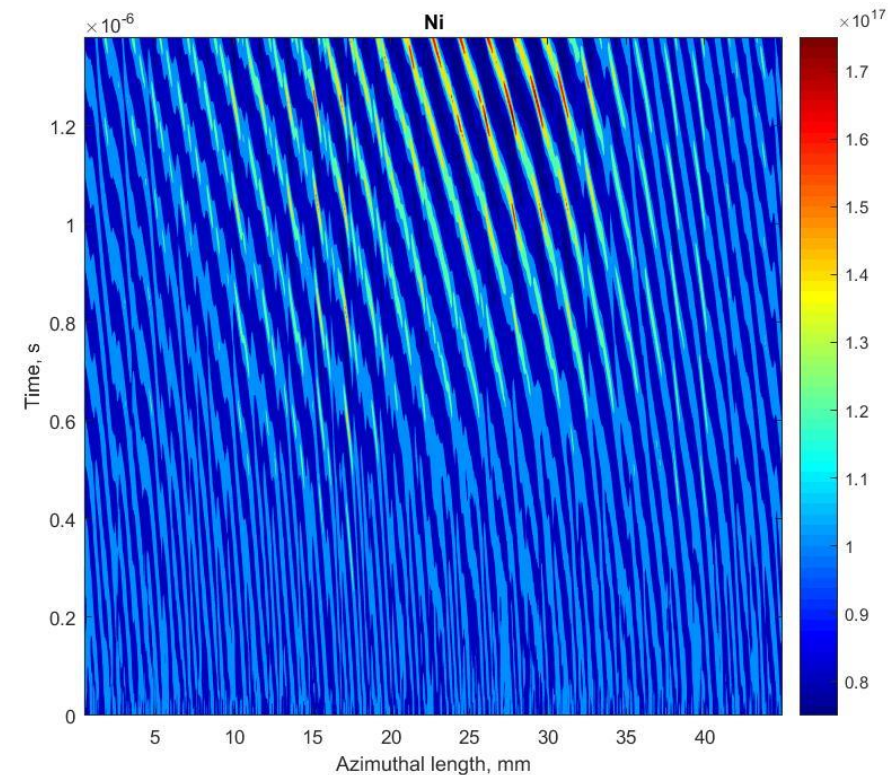


FIG. 1. Ion density as a function of time. Note the simultaneous appearance of the cnoidal structure along with modulation.

[Janhunen et al. PoP 2018]



Our simulation results using MPI-PIC simulation

Verification test for the wave-induced electron transport

- Lafleur reviewed the plasma-wave induced electron transport theory.

$$\langle n_e u_{ez} \rangle = -\mu_{\perp} (n_e E_z - \Omega \langle n_e E_y \rangle),$$

- In the limit of collisionless ($\nu_m \rightarrow 0$ hence $\Omega \rightarrow \infty$), the effective cross-field mobility is given by...

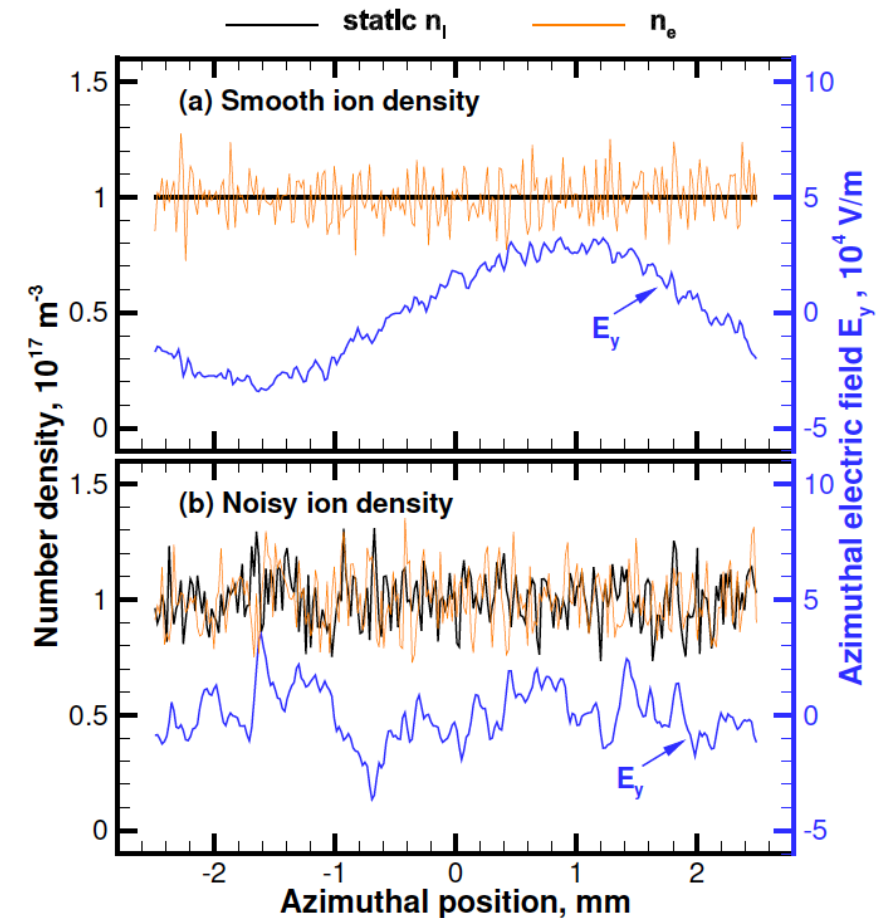
$$\mu_{\perp, \text{eff}} = -\frac{\langle n_e u_{ez} \rangle}{n_0 E_z} = -\frac{1}{n_0 E_z} \frac{\langle n_e E_y \rangle}{B}. \quad \langle Q \rangle = \frac{1}{T} \int dt \frac{1}{L_y} \int Q dy$$

- Using the Poisson equation, $\epsilon_0 \frac{dE_y}{dy} = e(n_i - n_e)$, for 1D azimuthal PIC simulation

$$\langle n_e E_y \rangle = \langle n_i E_y \rangle - \frac{\epsilon_0}{e} \left\langle \partial_y \left(\frac{1}{2} E_y^2 \right) \right\rangle \rightarrow \mu_{\perp, \text{eff}} = -\frac{1}{n_0 E_z} \frac{\langle n_e E_y \rangle}{B}.$$

Before looking into ECDI, what is the effect of ion density fluctuations (physical/numerical) to the electron transport?

- Theory shows that $\langle n_e E_y \rangle = \langle n_i E_y \rangle$ for a collisionless case. Hence, $\mu_{\perp,eff}$ is dependent on the **ion density modulation**.
- We propose a simple *verification* test case.
 - Turn off the ion dynamics (frozen ions)
 - Investigate effects of ion density modulation to the electron transport
- Two cases are compared.
 1. $n_i(y) = const. = n_0$ [smooth ion density]
 - $\langle n_i E_y \rangle = n_0 \langle E_y \rangle = 0$
 - Hence, $\mu_{\perp,eff} = 0$
 2. $n_i(y) \neq const.$ is initialized by macroparticles with randomized position [noisy ion density]



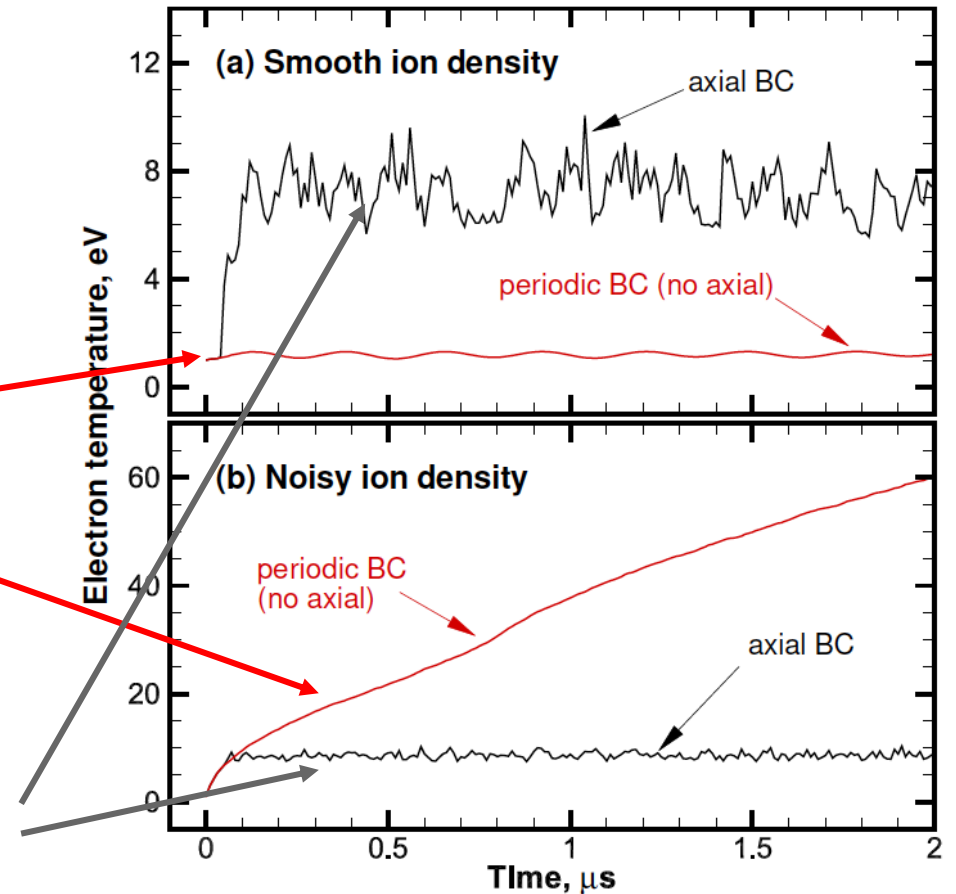
Hara, K. (unpublished).

Ion modulation itself + “bounded” BCs can excite electron transport without ECDI

- Electron energy equation (collisionless):

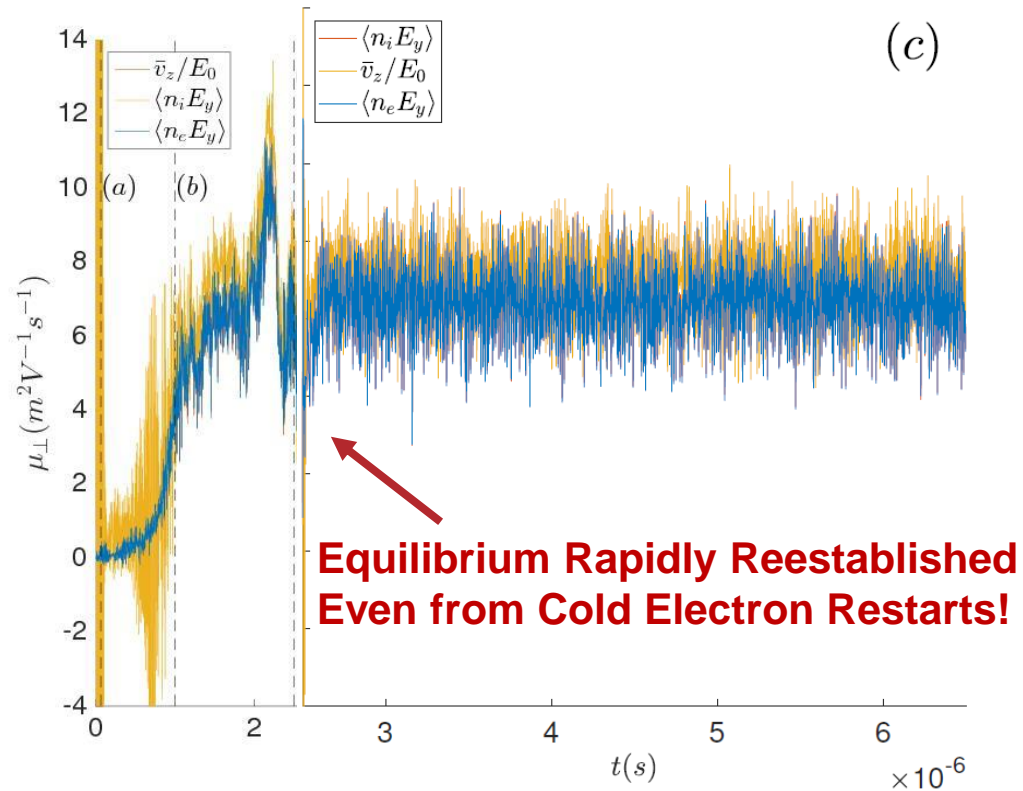
$$\frac{\partial}{\partial t} (n_e \epsilon_e) + \nabla \cdot (n_e \epsilon_e \mathbf{u}_e + p_{eV} \mathbf{u}_e) = n_e \mu_{\perp} E_z^2 - n_e u_{e\theta} E_{\theta}$$

- For **unbounded**, $\frac{\partial T_{eV}}{\partial t} = 2\mu_{\perp} E_z^2$
 - $\mu_{\perp} = 0$ (smooth n_i): $T_e = \text{constant}$
 - $\mu_{\perp} > 0$ (noisy n_i): T_e linearly increases
- For **bounded**, $\frac{\partial T_{eV}}{\partial t} + 2(T_{e0} - T_{e1}) \frac{u_{ez}}{L_z} = 2\mu_{\perp} E_z^2$,
 - $\mu_{\perp} > 0$ (T_{eV} saturates, because convective heat flux balance with cross-field transport)



Hara, K. (unpublished).

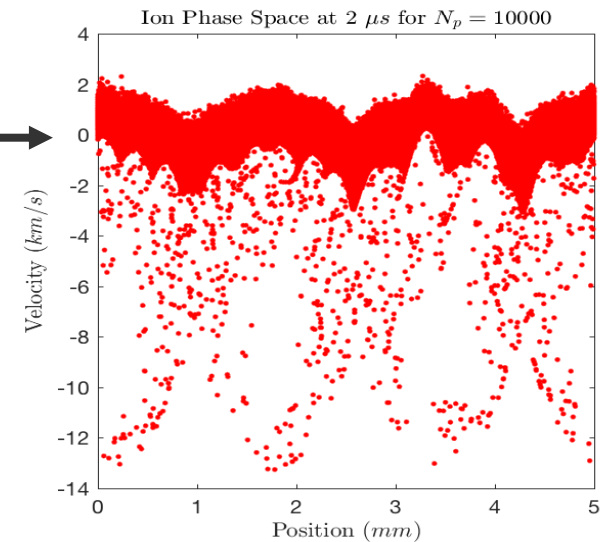
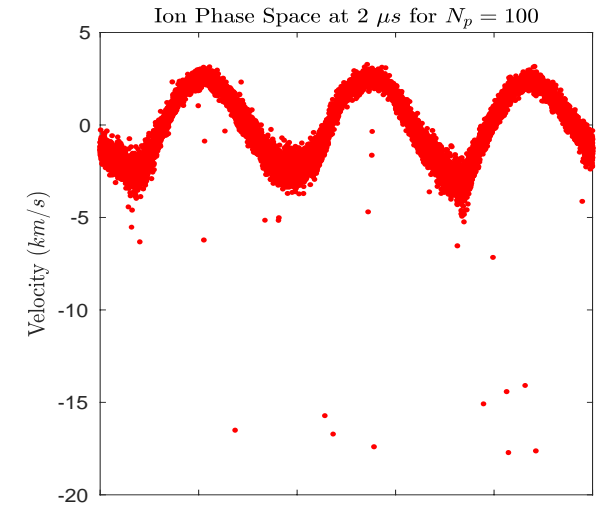
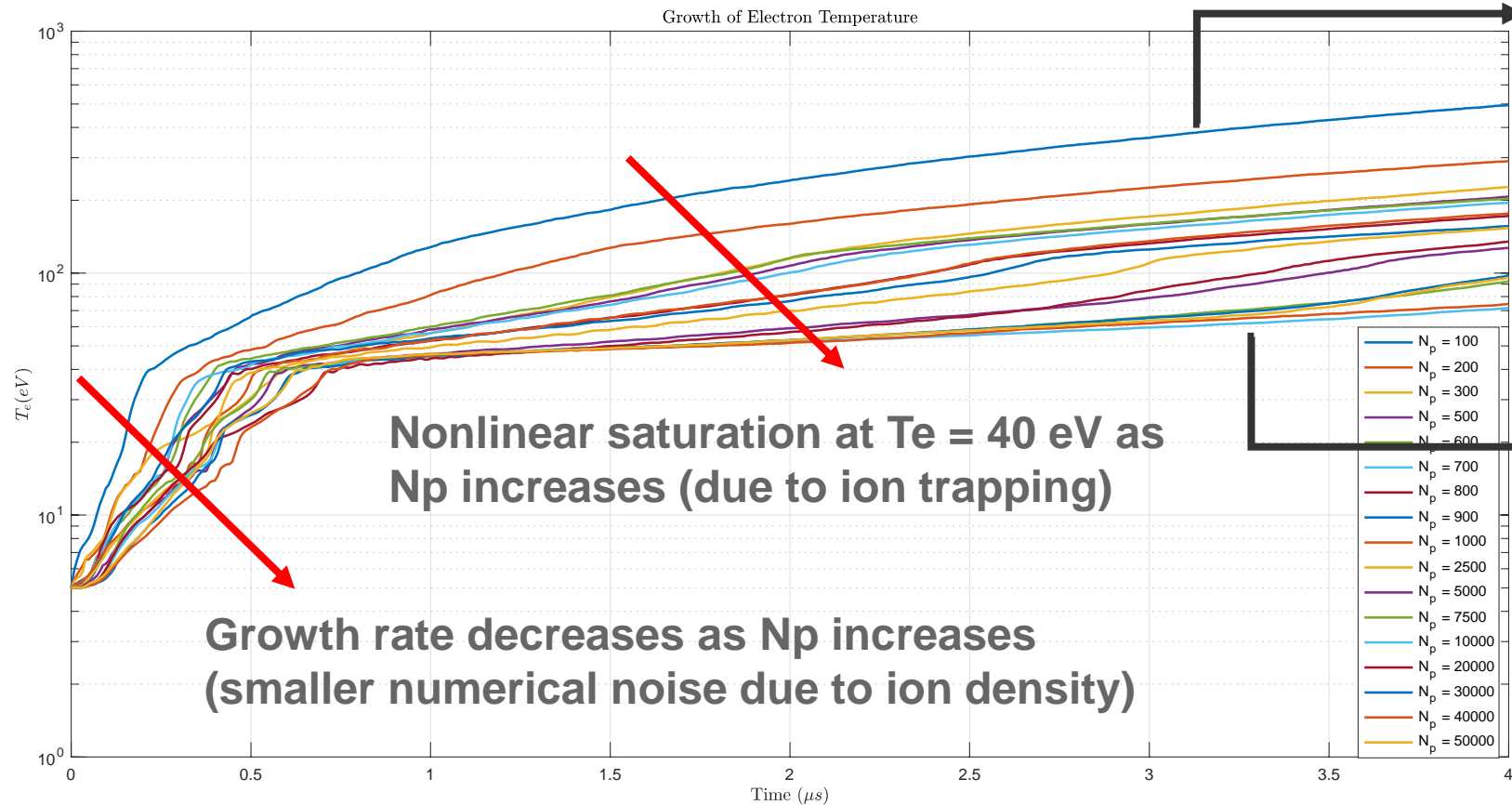
Mobility Estimates: Ions Frozen at Point



- Ions were Frozen and Electron Dynamics were Restarted
- Many Reduced HET Models Assume: Scale Separation τ_e vs. τ_i
- Still anomalous electron transport is observed.
 - Also $\langle n_i E_y \rangle = \langle n_e E_y \rangle$ is shown
 - Can we use this in a multifluid approach (coupling electron PIC with a multifluid ion/electron solver)

ECDI simulations with small domain ($L_y=5$ mm) and **unbounded** axial BC: N_p (# or particles/cell) = 100 - 50,000

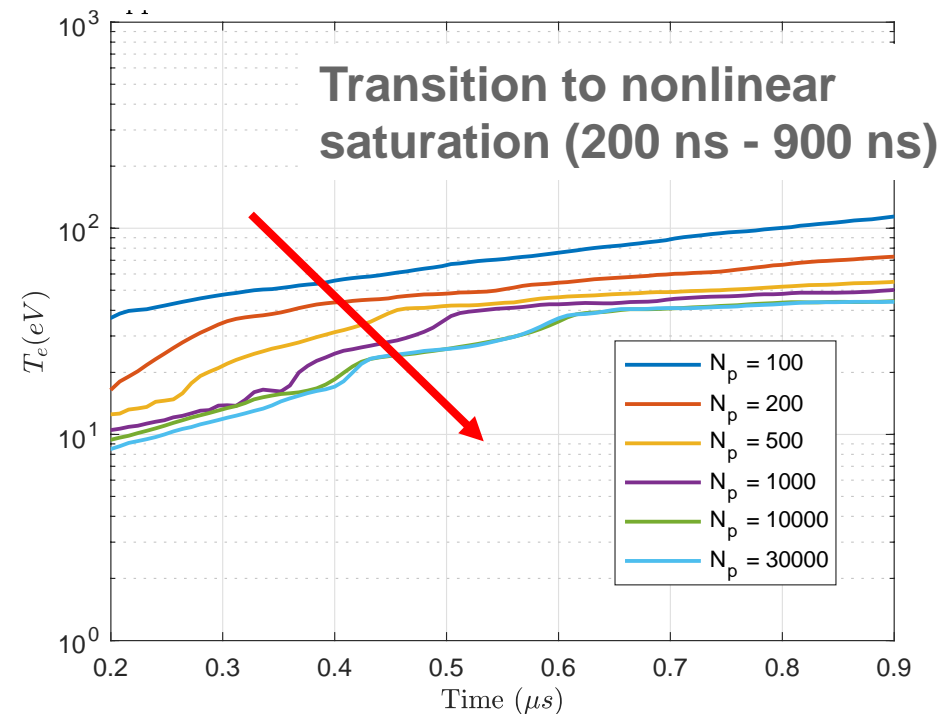
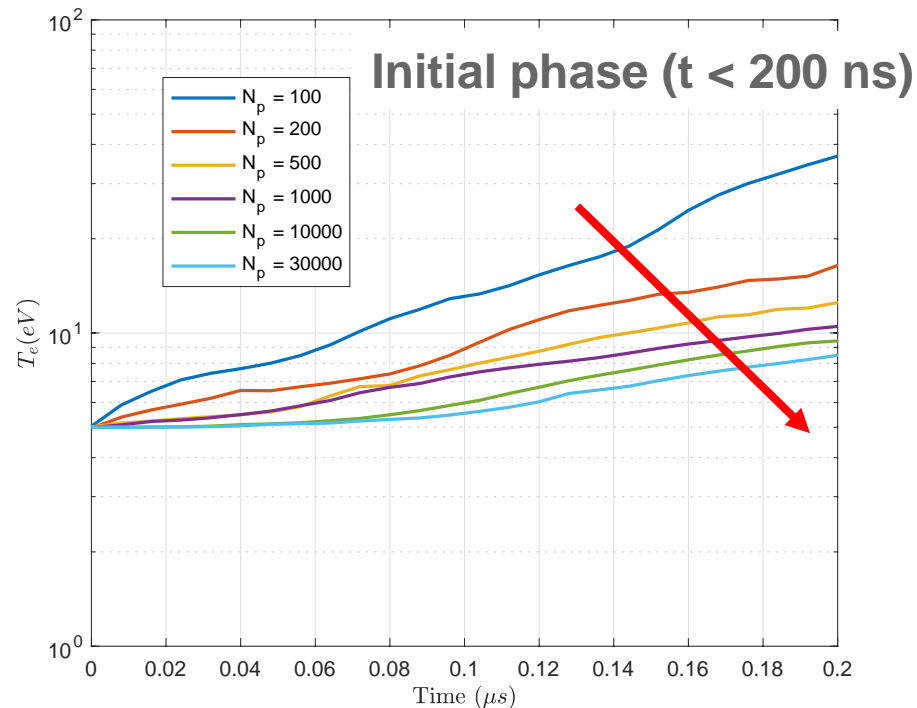
$$\frac{\partial}{\partial t} \int n_e \epsilon_e dV = \int n_e u_z E_z dV - \int n_e u_{e\theta} E_\theta dV$$



Cf) typically in one cell, 10^8 - 10^{10} real particles

Increasing macroparticle count reduces numerical noise

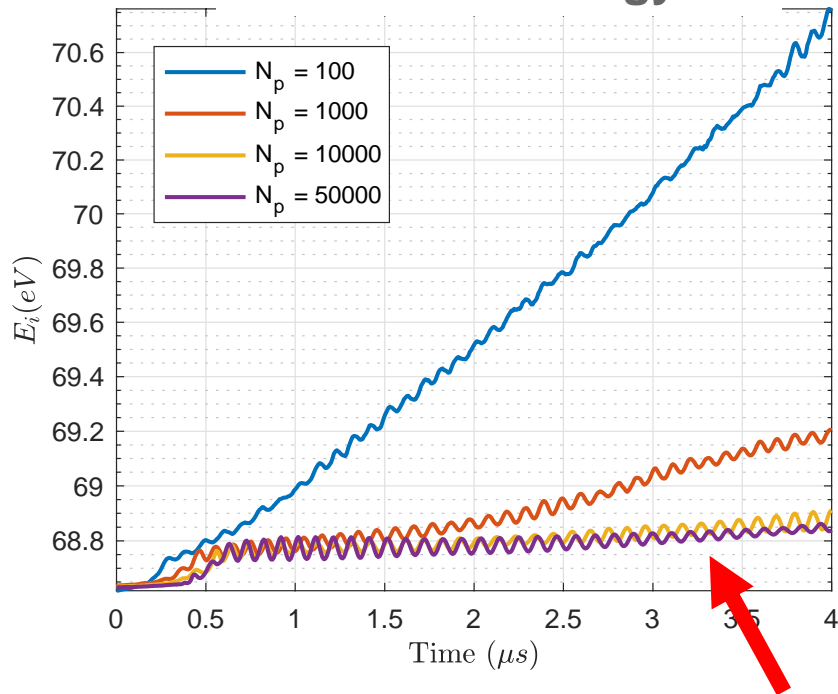
- The larger N_p , the slower instability growth starts, and the smaller growth rate.
- This is consistent with the “noisy ion density” case with the verification test case, ultimately approaching convergence (?) for $N_p \rightarrow \infty$.



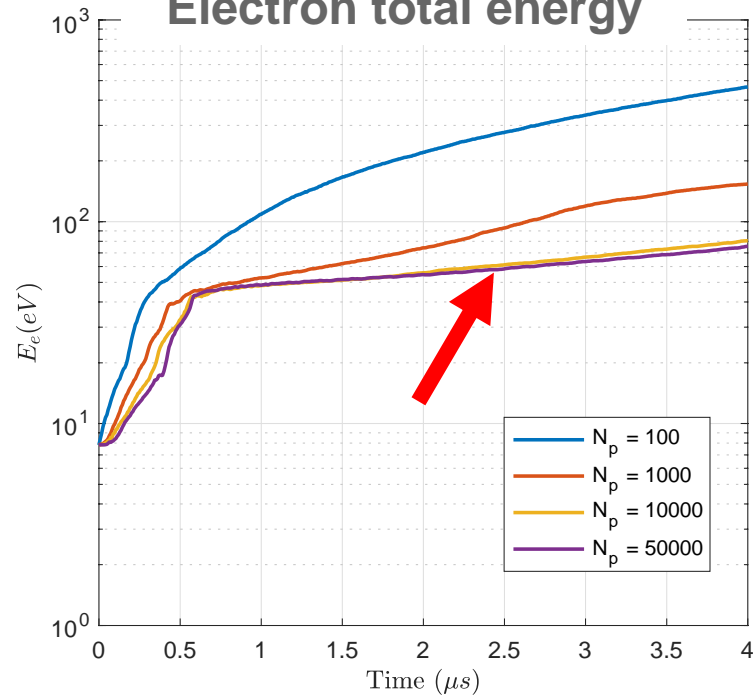
Energy growth: ions total energy, electron total energy, and maximum electric field (potential energy)

- Numerical heating is large for small N_p . Numerical heating is still present at larger N_p .
- Increase in energy is consistently present even at nonlinear saturation => **Numerical heating?**

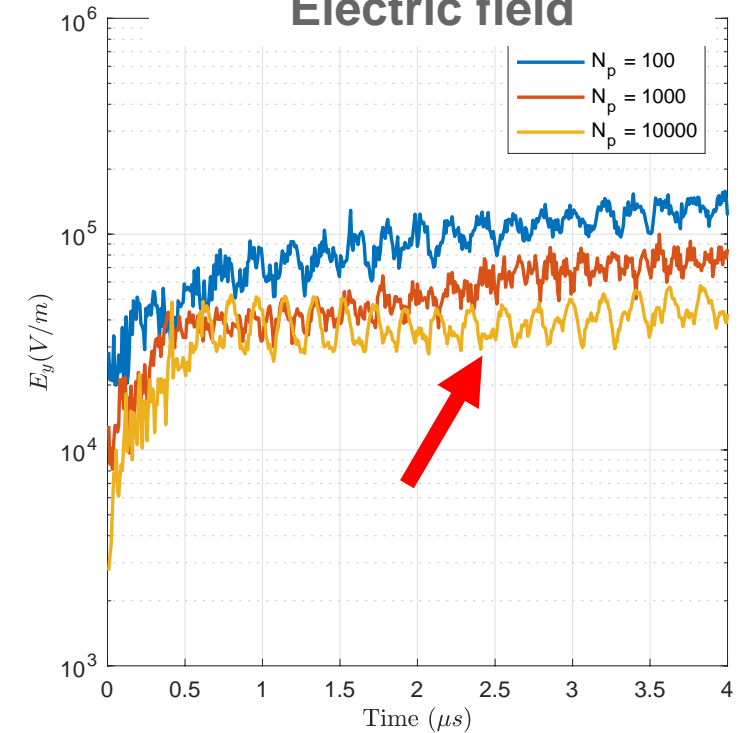
Ion total energy



Electron total energy

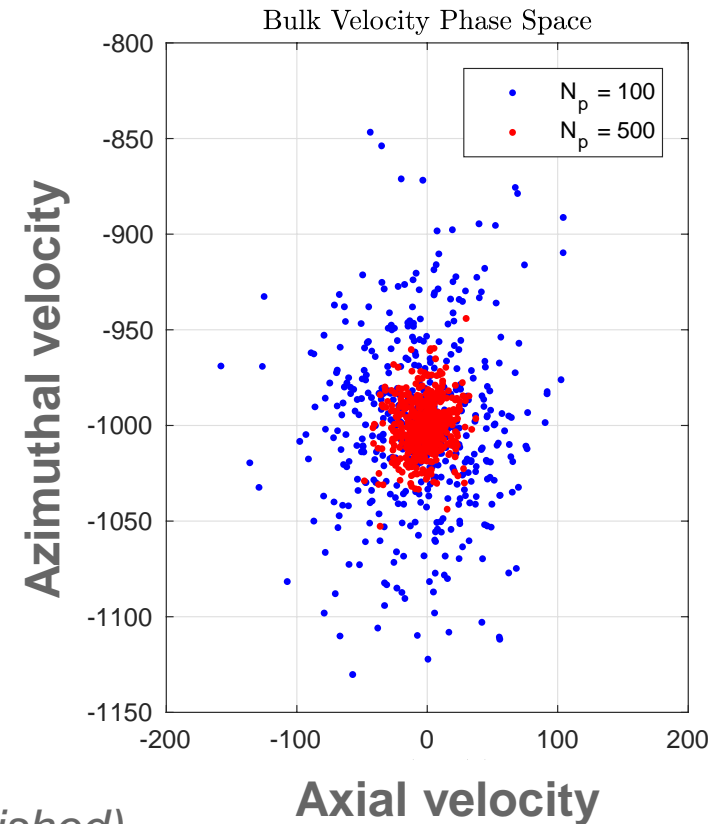
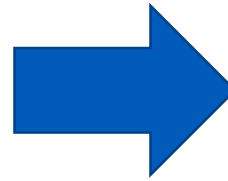
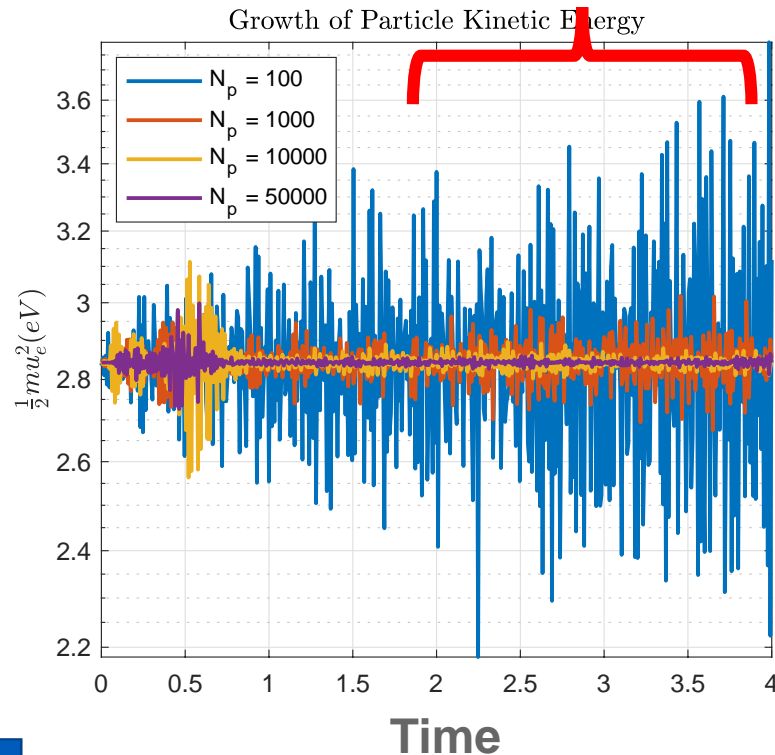


Electric field



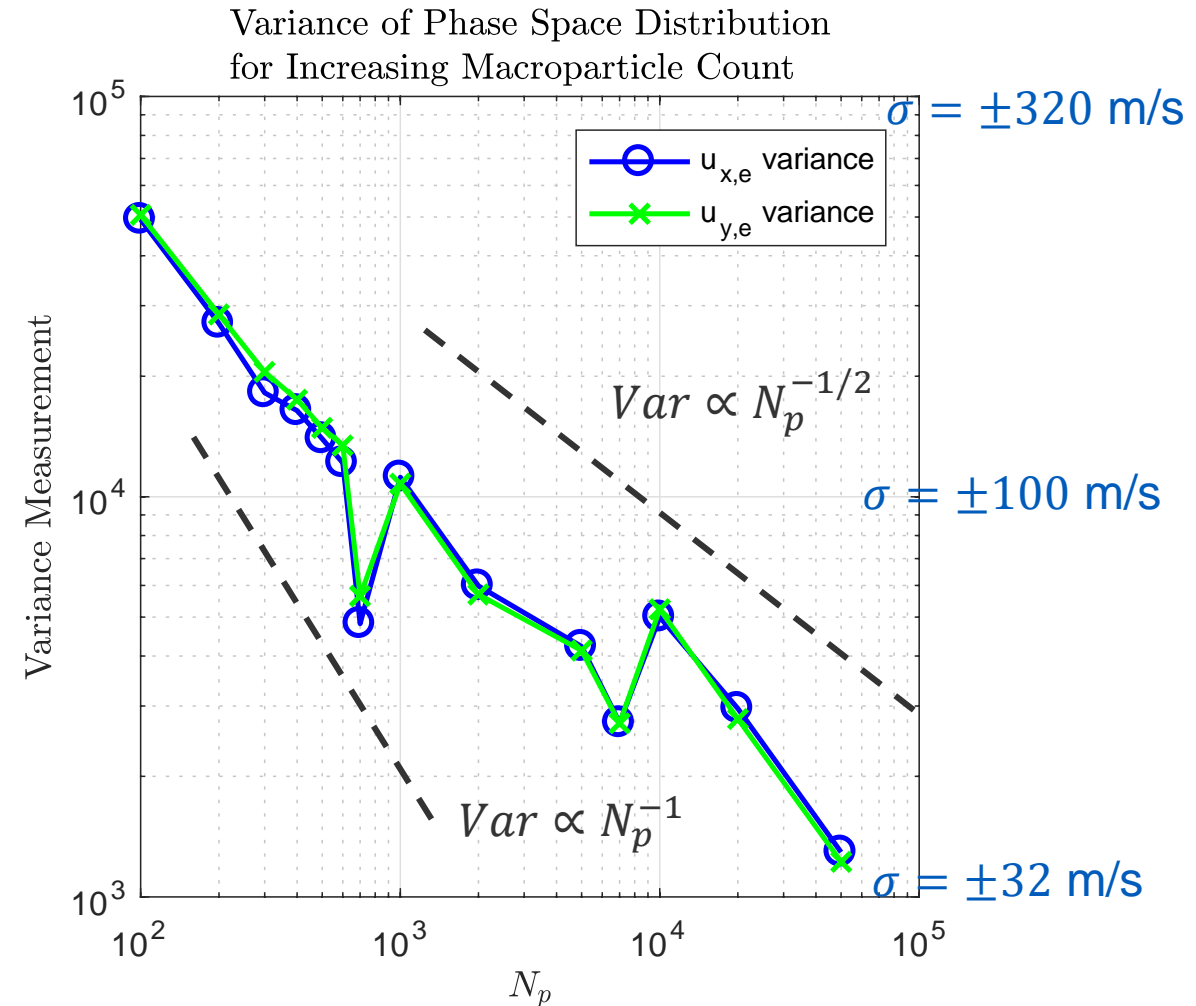
A measure for benchmarking codes: numerical convergence

- Macroscopic quantities can be used for benchmarking purposes of numerical codes and understanding numerical convergence?
- A phase space of spatially-averaged $u_{ex}(t)$ and $u_{ey}(t)$ is constructed from the nonlinear saturation region.



Statistical error vs Np: convergence? (1)

- PDF of $u_{ex}(t)$ vs. $u_{ey}(t)$ is constructed; and investigate the variance and covariance.
 - Standard deviation: $\sigma_j = \pm \sqrt{Var(v_j)}$
- A general trend of $N_p^{-1/2}$ convergence is shown.
- **Questions:**
 - Where can we claim that **numerical convergence** is achieved?
 - It seems like the results are not fully converged (e.g., hp convergence & round-off error, in CFD)
 - What is the **measure** to use for convergence? (e.g., variance, covariance)

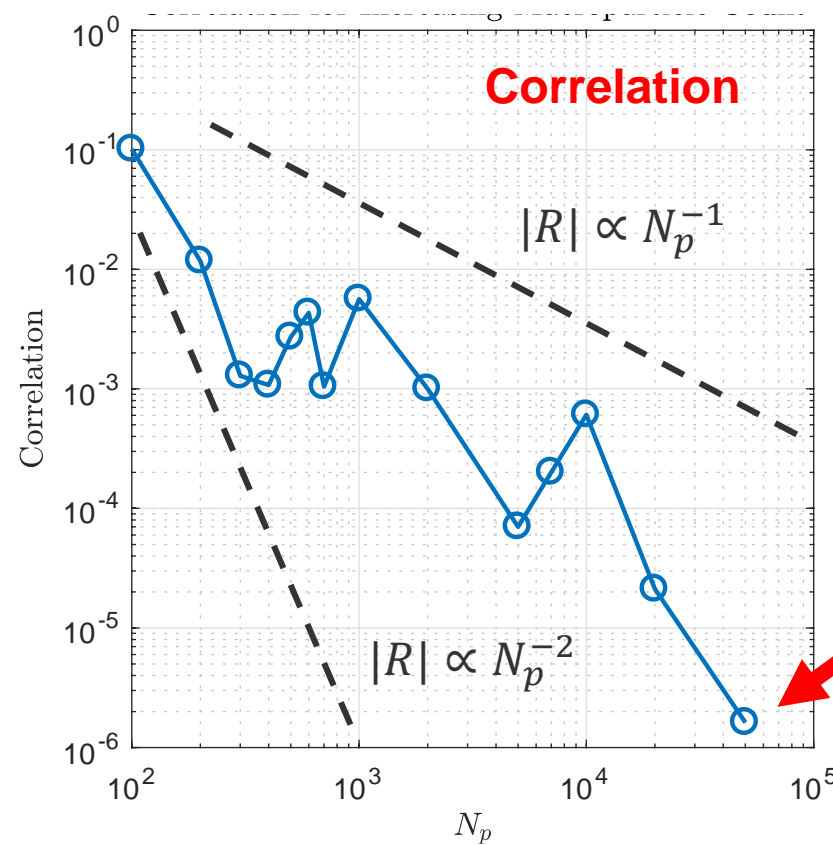
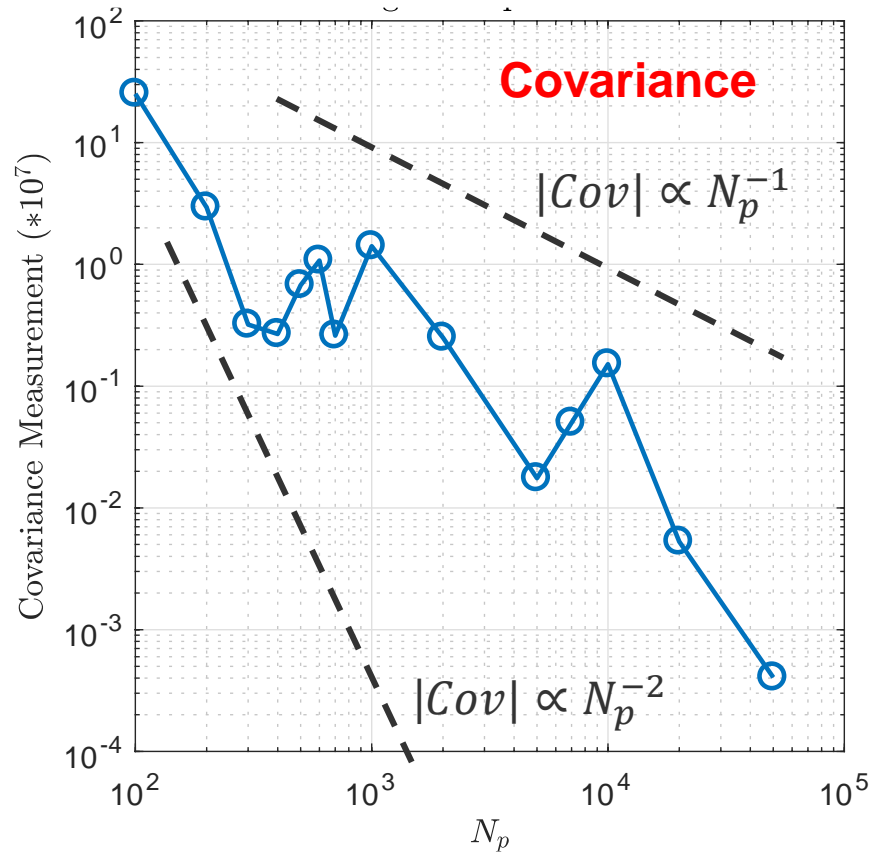


Hara, K. (unpublished).

Statistical error vs Np: convergence? (2)

$$\text{cov}(X, Y) = \frac{1}{n} \sum_{i=1}^n (x_i - E(X))(y_i - E(Y)).$$

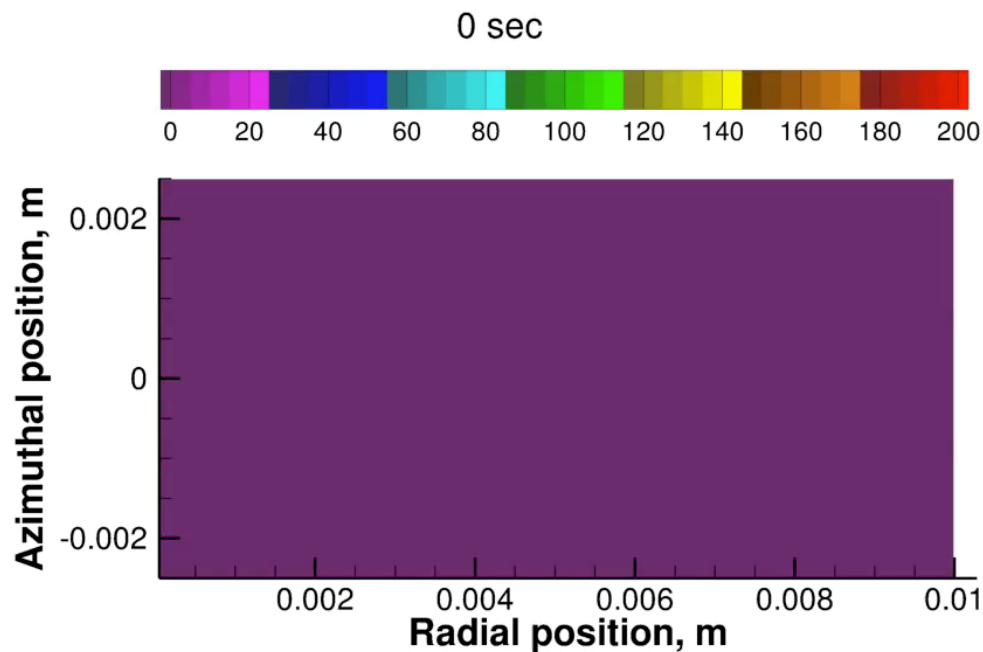
$$R = \frac{\text{cov}(X, Y)}{\sigma_X \sigma_Y}$$



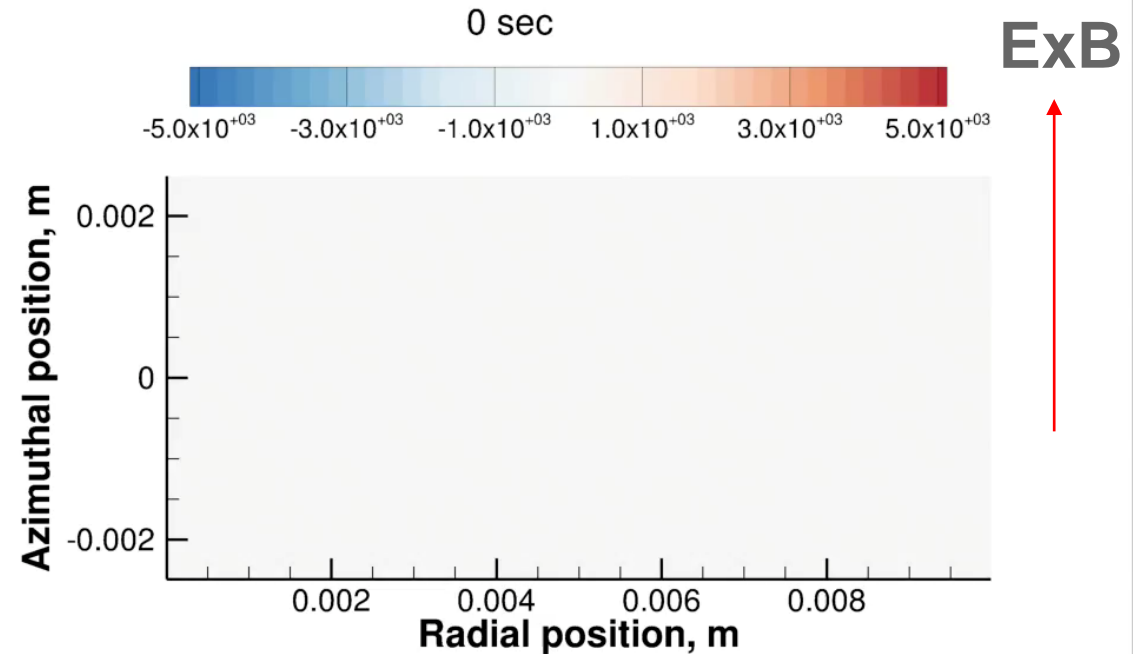
Approaching zero
“correlation”
between u_{ez} and u_{ey}
is good?

2D simulations for cosine ion density profile (1/2)

- Multidimensional effects (wave structures in sheath / ion front bowing out)
- Note $\phi = 0$ V (ref. potential) is assumed at northeast corner of the domain.



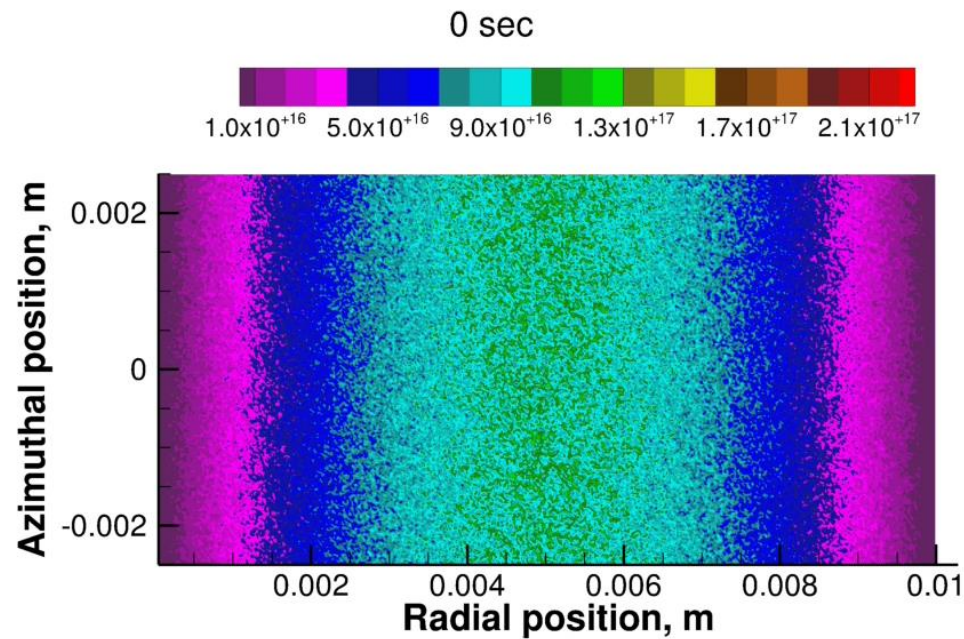
Potential (ϕ)



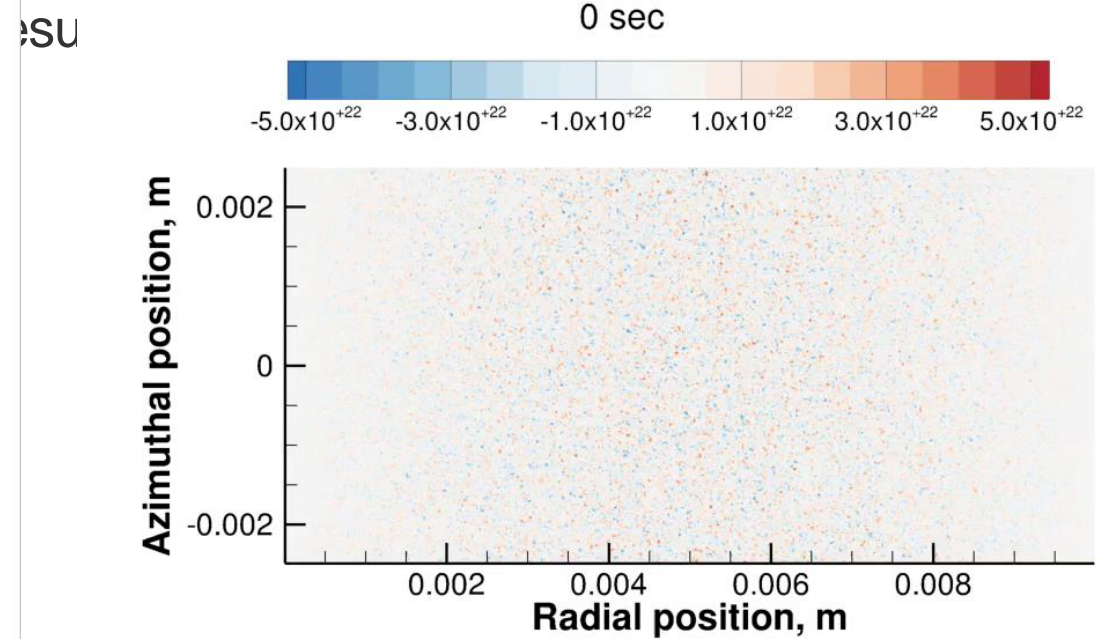
Ion azimuthal mean velocity (U_{yi})

2D simulations for cosine ion density profile (2/2)

- Coupling between “azimuthal” plasma wave and “radial” wall sheath.
- Radial electron flux is no longer locally zero, leading to radial Joule heating/cooling.



Plasma density



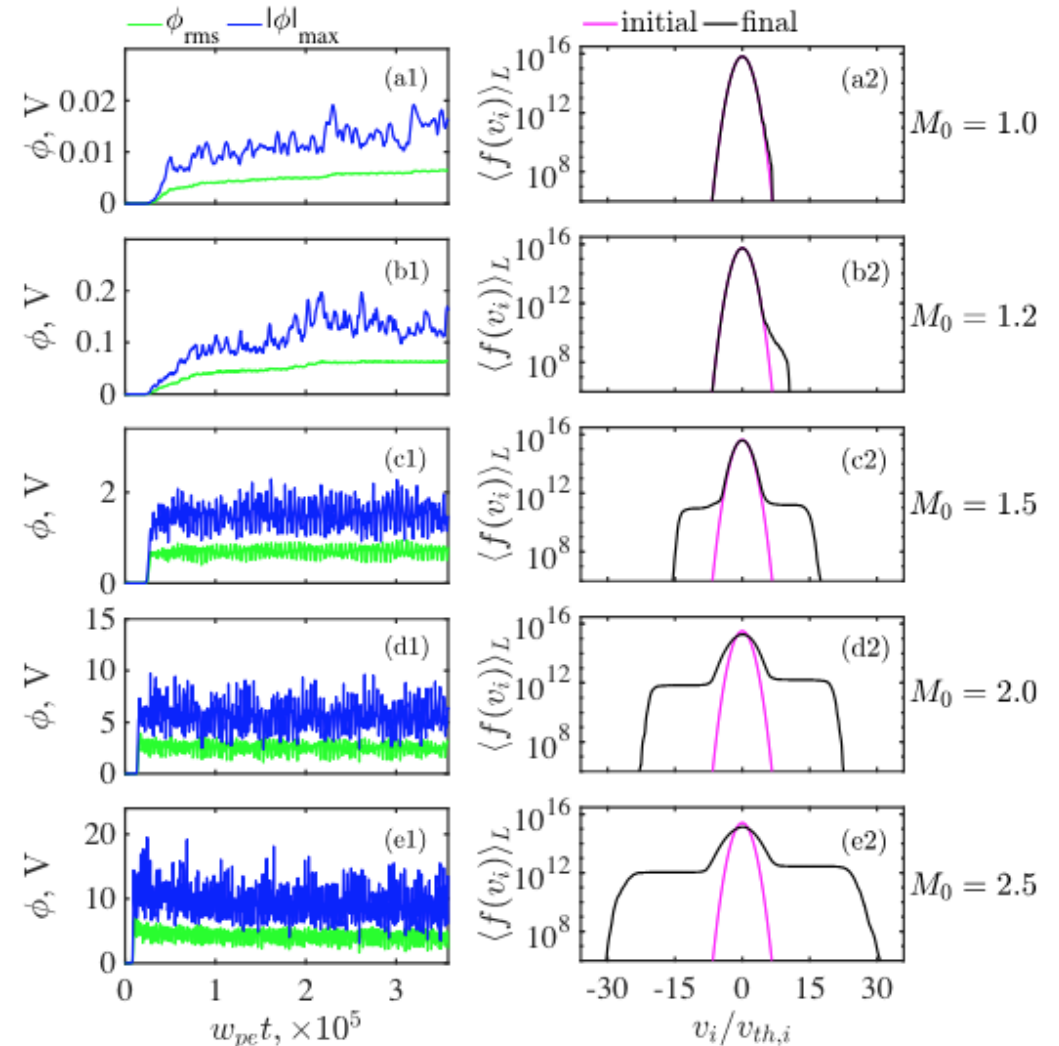
Electron radial flux ($n_e U_{xe}$)

ExB



Current-driven ion acoustic instability

- Electrostatic current-driven instabilities using noiseless grid-based direct-kinetic (DK) simulation for the Vlasov Poisson system. [Tuesday poster in GEC]
 - Generation of high-energy ion population (backward propagating) is observed at $M_0 = \frac{u_e}{v_{th,e}} \geq 1.3$
 - High-energy ions are 3-5 orders of magnitude smaller than bulk = at least $N_p \geq 10^5$ is needed if PIC is used.
 - We can evaluate sputtering rates etc from the set of ion VDFs obtained.
- A grid-based kinetic simulation of ECDI can be helpful for benchmarking?**



Future (and Current) Work

- **Comparing $\langle n_e \rangle$ with Boltzmann n_e**
- **Simple Experimental Evidence?**
Has v_θ -tail been observed in LIF?
- **Realistic Collision Models**
DSMC for Neutral/Ionize Charge-Ex
ES-PIC and 1D2V Coulomb Collisions
Tested on ES-Shock vs. Fluid Models
- **Multiscale Methods \rightarrow Full 3D?**
Adapt Quasi-1D Hybrid Codes for
Bursts of Electron Kinetics to Estimate μ_\perp ?
- **V&V for Dynamical Systems**

